Pyrolysis of Palm-oil Empty Fruit Brunch for Hydrogen Production Over Fe-doped Morphology Dependent NiO Nanomaterial

by

Basem Mohammed Ali Ali

14988

Dissertation submitted in partial fulfilment of

the requirements for the

Bachelor of Engineering (Hons)

(Chemical)

Jan 2015

Universiti Teknologi PETRONAS

Bandar Seri Iskandar

32610 Tronoh

Perak Darul Ridzuan

CERTIFICATION OF APPROVAL

Pyrolysis of Palm-oil Empty Fruit Brunch for Hydrogen Production Over Fe-doped Morphology Dependent NiO Nanomaterial

by

Basem Mohammed Ali Ali

14988

Dissertation submitted in partial fulfilment of
the requirements for the
Bachelor of Engineering (Hons)
(Chemical)

Approved by

_____

(Dr.Sujan chowdhury)

UNIVERSITI TEKNOLOGI PETRONAS

TRONOH, PERAK

Jan 2015

CERTIFICATION OF ORIGINALITY

This is to certify that I am responsible for the work submitted in this project, that the original work is my own except as specified in the references and acknowledgements, and that the original work contained herein have not been undertaken or done by unspecified sources or persons.

_____

(Basem Mohammed Ali Ali)

ABSTRACT

After successfully synthesized the nickel oxide catalyst with the hexagonal crystal shape and also the doping of different weight percent of iron, characterization of the catalyst has been done using TEM, FSEM, BET and etc. The effectiveness of the synthesized catalyst was demonstrated through the conversion of empty fruit brunches (EFB) into bio oil with presence of 5 different catalyst NiO, 1 wt%, 5 wt%, 10 wt% Fe-doped nickel oxide and one experiment without catalyst

The catalytic slow pyrolysis method was used to determine and predict the optimum weight percent of Iron doped with nickel oxide at the conditions of 60 ml/min of nitrogen flow rate, temperature of 400^{o}C. The results show the effects of the iron in producing hydrogen in the pyrolysis reaction, where the highest hydrogen amount produces where with 5 wt% Fe-NiO the optimum selectivity of hydrogen was 0.65 %. On the other hand the liquid yield of 39.80 wt% was obtained from the 10 wt% Fe-NiO catalyst.

ACKNOWLEDGEMENT

While it may be inspiration that starts this, it's the dedication of the folks that surround me that turn such an inspiration into a finished memoir. Without them, the end of the road might not be as near as I ever imagined. Having them around ensures the continuity of this training that I had been doing till the accomplishment of it. I would like to take this opportunity to express and extend my most sincere gratitude and appreciation to those who have been involved in the progress and process of this Project. All the help, the guidance and the encouragement that have been given are much appreciated.

A million thanks humbly addressed to a few highly respected individuals for whom without the inspiration and motivation given without hoping anything in return; the success of this Project would not be as what I was expecting. I would like to extend my heartfelt gratitude to my project supervisor **Dr Sujan Chowdhury** who has driven and supervised me throughout the entire journey upon completion of this Final Year Project.

I would like to acknowledge the laboratory facilities of this university which provide the materials, equipment and workplace throughout the project. Thanks to all laboratory technicians and also laboratory technologist for giving me support and sharing valuable information and knowledge. Without them, my project can't be done in time period and not to forget my friend **Mohd Aliffirham** who helped me the most to finish the lab experiment.

I would like also to acknowledge my lecturers' contributions that have also assisted me throughout this training by providing us enlightenment on areas of confusion without expecting anything in return.

Lastly, I would like to gives my special gratitude to my parents for all the supports and encouragement.

TABLE OF CONTENTS

Tables

Figures

CHAPTER 1

INTRODUCTION

1.1 Background

The increase of world population has led to a number of challenges that face us all. As stated in bp statistical review of world energy 2014 the year 2013 saw an increase in growth of global energy consumption, the growth nearly 100 % over the past decades. Transportation sector is the main field of energy consumptions constituting about one fifth of the total and this requirement depletes crude oil reserves (Sorrell, Speirs, Bentley, Brandt, & Miller, 2010; van Ruijven, van Vuuren, & de Vries, 2007) A build-up of greenhouse gases induces a global climate change causing long droughts in some places and severe flooding in others. These changes in the natural world increase pressure on ecosystems, leading to a loss of biodiversity. In the latest report by the IPPC, the international panel on climate changes, we see the contribution of different fossil resources on the concentration of CO_2 in the atmosphere.

Sustainable sources of energy are needed in the near future, Bio-fuels produced from renewable recourses has attracted attention and interest. The aim of current researches is to produces bio-hydrogen by pyrolysis reaction and transfer renewable biomass resources to liquid fuel that is suitable for the transportation and the tangible products such as paints, plastic and pharmaceuticals (De, Saha, & Luque, 2014; Huber, Iborra, & Corma, 2006).

Biomass derived fuel can be produced within a relatively short cycle and that makes to be the perspective fuel of tomorrow (Balat, 2011). Flash paralysis is the most widely used process for production of bio-oil, as this has been found as feasible route; which is a densification technique where both the mass-and energy-density is increased by treating the raw biomass at intermediate temperature (300-600 ^{o}C) within high heating rates and short residence times (Huber et al., 2006).

1.2 Problem statement

The perspective fuel of tomorrow –bio-fuels – will play an important in our energy future to reduce our dependence from petroleum derived resources and achieve the changes required to address the impacts of global warming as well. Latterly much attention has been focused on identifying suitable biomass species, which can provide high-energy outputs,(McKendry, 2002).

Large amount of palm oil waste in Malaysia, US and some of the European countries which is hard to be disposed and there has been great development relating to the conversion, crop production, etc. All this promise the application of biomass at a lower cost and higher conversion efficiency than was possible previously. statistical review of world energy (2014).

Biomass also a great source of hydrogen which considered is an attractive alternative to fossil feedstock because of essentially zero net CO_2 impact.(Mann, Chornet, Czernik, & Wang, 1994). However, optimization of hydrogen production from biomass need to be optimized by developing suitable catalyst.

1.3 Objective

- To synthesize and characterize the Nickel oxide with hexagonal microstructure.
- To synthesize and characterize the Nickel oxide impregnated with Iron
- To find effective concentration of iron metal for the doping Nickel oxide.
- To produce hydrogen and bio-oil via pyrolysis from biomass wastes.

1.4 Scope of the study

The scope of the study is to finding effective concentration of Iron and metal to be impregnated with Nickel oxide. After that iron and will be impregnated with nickel oxide nanostructure. The physical and chemical characteristics and morphology of the nickel oxide and iron-doped nickel oxide is investigated using TEM, FSEM, XRD, BET, and RAMAN. The prepared catalysts will be used for pyrolysis which will optimize hydrogen production.

CHAPTER 2

LITERATURE REVIEW

Considerable effort and research has been directed toward the process of producing liquid fuel and hydrogen form biomass. the products resulted from biomass is less efficient compare with the conventional fuel oils, So substantial research also carried out in order to optimize the production of bio-oil and hydrogen. For the purpose of this work literature review is divided to the following:

2.1 Pyrolysis oil

Flash Pyrolysis is the most widely applied process for producing bio-oil. Pyrolysis oil or bio-oils is a dark brown, free flowing with smoky odor liquid from biomass pyrolysis. There are complex mixtures of more than 300 compounds. The major organic compounds are acids, alcohols, ether, ketene, aldehyde, phenol, ester, sugar, furan, and nitrogen compound (Czernik & Bridgwater, 2004; Huber et al., 2006). The major components of biomass are cellulose, hemicelluloses, and lignin (White, Catallo, & Legendre, 2011).

The negative chemical properties; such as the complex mixtures of chemical compounds and high oxygen content has resulted instability of bio-oil. Czernik and Bridgwater (Czernik & Bridgwater, 2004) have presented the typical properties of bio-oil and compare them of that of heavy fuel-oil.

The oxygen content in bio-oil is very high 35-50 wt% this content of oxygen affects the homogeneity, polarity and heating value (HV). That is less than 50% of that of conventional fuel oils. Water content also present up to 30 wt % which has both negative and positive properties as stated by (Czernik & Bridgwater, 2004) it lowers the heating value on the other hand improves bio-oil flow characteristics. The pH of bio-oil indicates the presence of acetic and formic acids which constitutes a problem as it will initially harsh the equipments used. The following table shows the difference of the properties between bio-oil and fuel-oil.

Table 1 Typical Properties of Bio-oil and of Heavy Fuel Oil

physical property	bio-oil	heavy fuel oil
moisture content, wt %	15−30	0.1
pH	2.5	−
specific gravity	1.2	0.94
elemental composition, wt %		
C	54−58	85
H	5.5−7.0	11
O	35−40	1
N	0−0.2	0.3
ash	0−0.2	0.1
HHV, MJ/kg	16−19	40
viscosity (at 50 °C), cP	40−100	180
solids, wt %	0.2−1	1
distillation residue, wt %	up to 50	1

2.2 Bio-oil upgrading

The most significant problems of bio-oil as a fuel are poor volatility, high viscosity, cold flow, and corrosive problem. The main concern for burning bio-oil is diesel engines have to do with difficult ignition (due to low HV and high water content) (Huber et al., 2006). Bio-oil must be upgraded if they are to be used as a replacement for diesel and gasoline fuels. There are three different routes for upgrading bio-oil (1) zeolite upgrading (2) forming emulsions with the diesel fuel and (3) Hydrodeoxygenation with typical catalysts which considered as the most effective method. Hydrodeoxygenation (HOD) improves the effective H/C ratio. The key challenge of HDO processes is to achieve high degree of oxygen removal with minimum hydrogen consumption, for which catalysts need appropriate and careful design (De et al., 2014)

Precious metal catalysts (e.g. Pd, Pt. Re, Rh and Ru) and non-precious metal catalysts (e.g. Fe, Ni, and Cu) have exhibited good activates in Hydrodeoxygenation reaction (Bykova et al., 2012). HDO of bio-oil involves the presence of catalyst and hydrogen at moderate temperature (300–600 °C). The following schematic represent the HDO reaction; oxygen is removed in the form of water.

$CH_2O + H_2 \rightarrow CH_2 + H_2O$ *Where* CH_2O *reperents carbohyrate in bio oil*

2.3 Metal based Catalysts

The development of catalysts for upgrading was based on the idea of bifunctional process. Oxy-groups in the oxygen-containing compound in bio-oil need to be activated by oxide from transition metal with variable valence. On the other hand , a transition metal in it reduced state is require to activate the dihydrogen; HDO reactions require at least two types of active sites (Yakovlev et al., 2009).

Yakovelv (Yakovlev et al., 2009) also found that Ni-Cu had the potential to completely eliminate the oxygen content in anisol as the reaction performed in fixed bed reactor at temperature range of 250 to 400 ^{o}C and pressure of 5 to 20 bar. He also mentioned that the Ni-Cu is more active than single Ni catalyst. Since HDO of bio-liquids is expected to be a large-scale process, employment of noble metal-based catalysts could significantly raise production costs. Thus, it seems more reasonable to use Ni-based catalysts for bio-oil HDO due to their high activity for hydrogenation and lower cost (Zhang, Wang, Ma, Zhang, & Jiang, 2013)

In (Wang et al., 2013) it is fond that high performance of the optimized Ni‑Co/Al_2O_3catalyst in the steam reforming of tar is suggested to be due to the synergy between Ni and Co atoms on the Ni‑Co alloy surface in the steam reforming of oxygenates.

2.4 Synthesis of Fe-doped Nickel oxide

There are a few methods in synthesizing the Fe-doped Nickel oxide one why was done by (Moura, Lima, Jesus, Duque, & Meneses, 2012) co-precipitation method. The nickel nitrate and iron nitrate queues solution were mixed and sodium hydroxide solution was used to control pH of 13. The resulting gels then were washed and centrifuged several times until remove the Na ions, and dried in air at 80 ^{o}C. The crystalline structures of the sample were investigated by X-ray. The following diagram shows the result of NiO without the presence of impurities and F-doped NiO; the X-ray shows identical structure of both NiO and F-doped Nickel. In the result also the SEM image show decrease in the particle size in doped sample differently crystalitte size; the particle microstrain increase with Fe insertion. (Moura et al., 2012) associate that to small difference between ionic radii of Ni^{2++}(0.69 A) and Fe^{3+}(64 A).

The results show uniform size tending to a nanorod-like shape for Fe-doped nickel. Both results of XRD and SEM show that the particle size decreases and there is a change in particle morphology as a function of Fe insertion.

Iron-doped nickel also was synthesized by ball milling at 2000 rpm for 20 min, by (Rahmatollah**,** 2012). The samples were prepared from $NiCl_2.4H_2O$ and $FeCl_3.6H_2O$ powder and citric acid. It was calcined at 550 ^oC for 5 h. The analysis of the samples using SEM shows uniform size of the Fe-doped NiO nanoparticles. The XRD also shows a well crystallized of the Fe-doped nickel oxide; no peaks phase of NiO or impurity peaks are observed.

2.5 Catalytic slow Pyrolysis

Currently great efforts have been directed to produce bio-fuel from agriculture resides; non-food/inedible "cellulosic" biomass feedstock. There are also researches on producing bio-fuel mainly from plant which is suitable for food. This is not suitable because some populations in the world suffer from hanger or malnutrition.

In a study conducted by (Dang, Yusup, Yoshimitsu, & Nuruddin, 2013) they have studied the optimization condition in producing bio-oil from rice husk. They have found that the highest liquid yield of 38wt% was obtained at the optimum conditions with temperature of 500^oC with nitrogen flow rate of 60ml/min and 12wt% of H-ZSM-5. The following diagram represents the comparison of the liquid Yield product with operating conditions of nitrogen flow rate of 60ml/min, temperature of 500^oC as an optimum conditions.

Figure 1: Yield of liquid product from (Dang et al., 2013)

2.6 Bio-oil derived from empty fruit brunches

Empty fruit brunches (EFB) is the major biomass byproduct from the palm OIL industry. EFB has a great potency as basic raw materials used for the fermentative production because they contain 37.3 – 46.5% cellulose, 25.3 – 33.8% hemicelluloses.

These cellulosic materials relatively inexpensive feedstock as being abundant and outside the human food chain makes and no conflict with the food supply.(Sudiyani et al., 2013)

In a research done by (Sudiyani et al., 2013) they have investigated the effect of variables such as reactor temperature in the range 425–550 °C and feedstock ash content in the range 1.03–5.43 mf wt% on washed and unwashed EFB. They have found that the yield maximum for liquids produced from washed EFB was increased to around 72% compared to just under 50% for liquids produced from unwashed EFB. The ash content of the feedstock has been found to significantly influence the yield of organics. The higher the concentration of ash in the feedstock the lower the yield of pyrolysis liquid.

2.7 Hydrogen from Biomass

Hydrogen is also an ideal clean energy that got a considerable attention to be produced from biomass. One of the methods used to produce hydrogen is gasification but it favors tar formation unless it is done at high temperature. Catalytic gasification of biomass is used to eliminate tar. (Inaba, Murata, Saito, & Takahara, 2006).

In this study also they found that in most cases, the higher reaction temperature led to a greater amount of hydrogen formed, a higher rate of gasification, and less tar formation and carbon deposition. They compared the hydrogen yield, at 500 °C ad 600°C, the hydrogen yield was not affected by Ce-loading, while at 600°C, the hydrogen yield was decreased by Ce-loading due to hydrogen combustion to H2O.

They concluded that in formation of hydrogen from cellulose, it appears that metallic Ni is the catalytically active site and there is minor structure sensitivity of Ni. Ce-loading enhanced the combustion activity of tar and improved the methanation activity of metallic Ni, raising the overall gasification rate.

CHAPTER 3

METHODOLOGY

The methodology to be adopted for achieving the desired objectives is:

Stage 1: Catalyst preparation

3.1 Activities

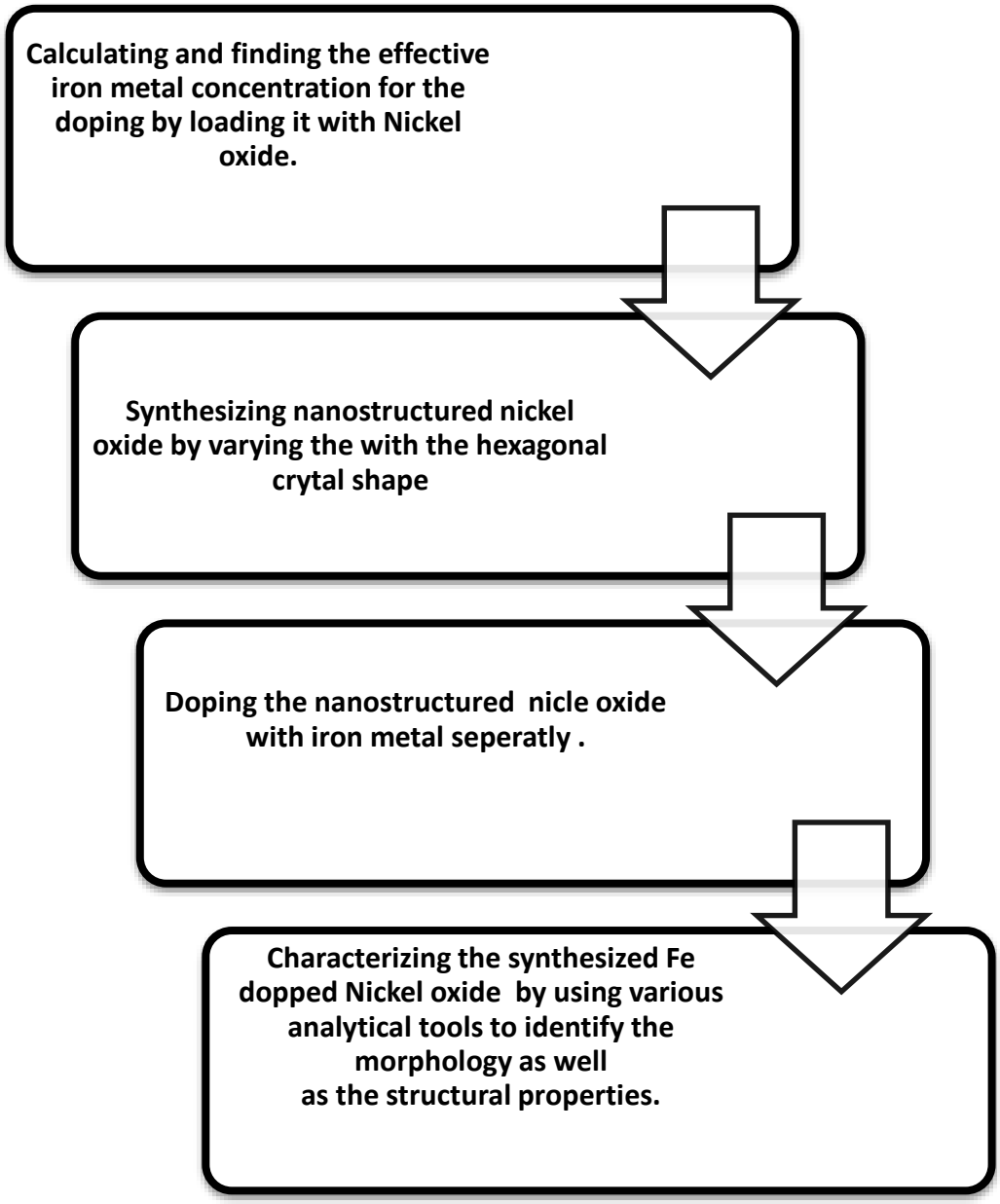

Figure 2 Activities

Stage 2: Testing the model and obtaining results

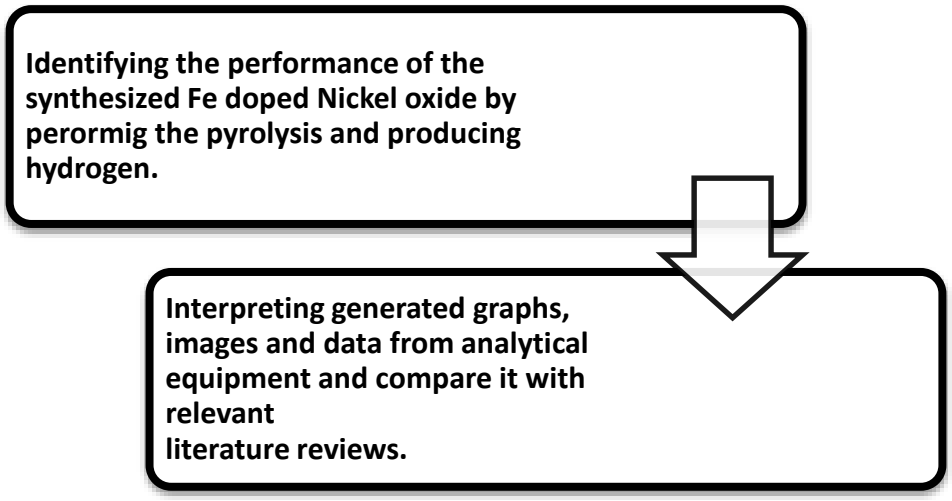

Figure 3 Testing model and obtaining result

3.2 Materials and Equipments

- Chemicals for Fe-doped NiO (nickel nitrate, iron nitrate, NaOH and Deionizedwater.
- Chemicals for Iron-doped nickel oxide (Iron nitrate)
- Biomass
- Semi-Bach reactor
- Thermocouple
- pH mater
- X-ray powder diffraction (XRD)
- Scanning Electron Microscope (SEM)
- Transmission electron microscopy (TEM)
- Surface Area Analyzer (BET)
- Raman Spectroscopy

3.3 Synthesizing of Nickel oxide NiO

Table 2 Synthesizing of Nickel oxide NiO

1	•24g of NaOH being immersed in 100ml of water. 100ml of 6 M of NaOH were prepared.
2	•Solution transferred to 100ml conical flask. Stored for a day and cooled down before using it.
3	•To produce 0.01 mol of nickel nitrate + sodium hydroxide solution , Nickel(II) hexahydrate, $Ni(NO_3)_2.6H_2O$ will be weighed for 2.91 g followed by 10 ml of NaOH and 15 ml of deionize water.
4	•Solution being out inside the teflon in auto-clave and being heat for 170˚ C for 24 hour.
5	•Solution is filtered using filtered pump before calcined it under nitrogen purging flow for 600˚ C for 5 hours.

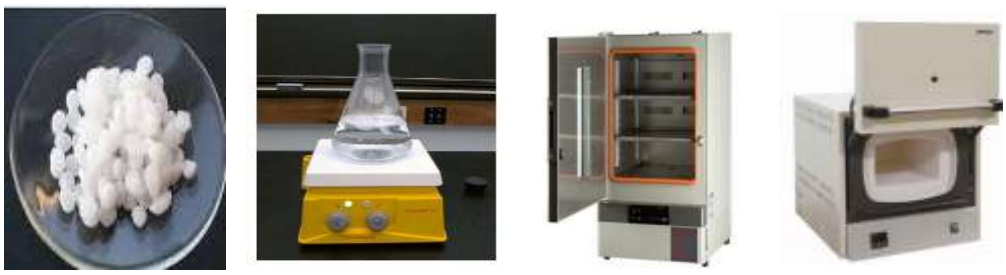

Figure 4 Synthesizing of Nickel oxide NiO

3.4 Impregnation of Iron with Nickel oxide

Table 3 Iron Impregnation with Nickel oxide

1	•Add 1 gram of Nickel oxide with 2 ml deionized water into a 50 ml beaker.
2	•Adjust the pH of the compound to pH 8 using Sodium Hydroxide.
3	•Add 2 ml of deionized water with (10 wt% =0.167 g / 20wt% = 0.375g) of Iron Nitrate Hexahydrate into the beaker containing NickelOxide compound.
4	•The mixure is stirred again for 30 minutes.
5	•The mixture was exposed to vacuum at room temperature for 3 h , and then dried 24 h at 373 K.
6	•The resulting impregnated solid was grounded and sieved (100–160 µm), and then calcined at 773 K under Argon flow (50 Nml/min) for 1 h.

Figure 5 Iron Impregnation with Nickel oxide

3.5 Gantt chart (FYP):

Table 4 Gantt chart

Project activities	Week No																														
	SEPT			OCT				NOV				DEC/JAN			Jan		Feb				Mar				Apr						
	1	2	3	4	5	6	7	8	9	10	11	12	13	14	1	2	3	4	5	6	7	8	9	10	11	12	13	14	15		
Selection of project topic																															
Preliminary research work																															
Submission of extended proposal																															
Proposal defense																															
Fine-tuning research methodology																															
Submission of interim draft report																															
Submission of interim report																															
NiO Catalyst preparation																															
Fe- doped NiO preparation																															
Submission of progress report																															
Characterization of catalyst																															
Data analysis and documentation																															
Pre-SEDEX																															
Catalyst application																															
Submission of dissertation																															
Submission of technical paper																															
Oral presentation																															
Submission of project dissertation																													X		

3.6 Slow Catalytic Pyrolysis

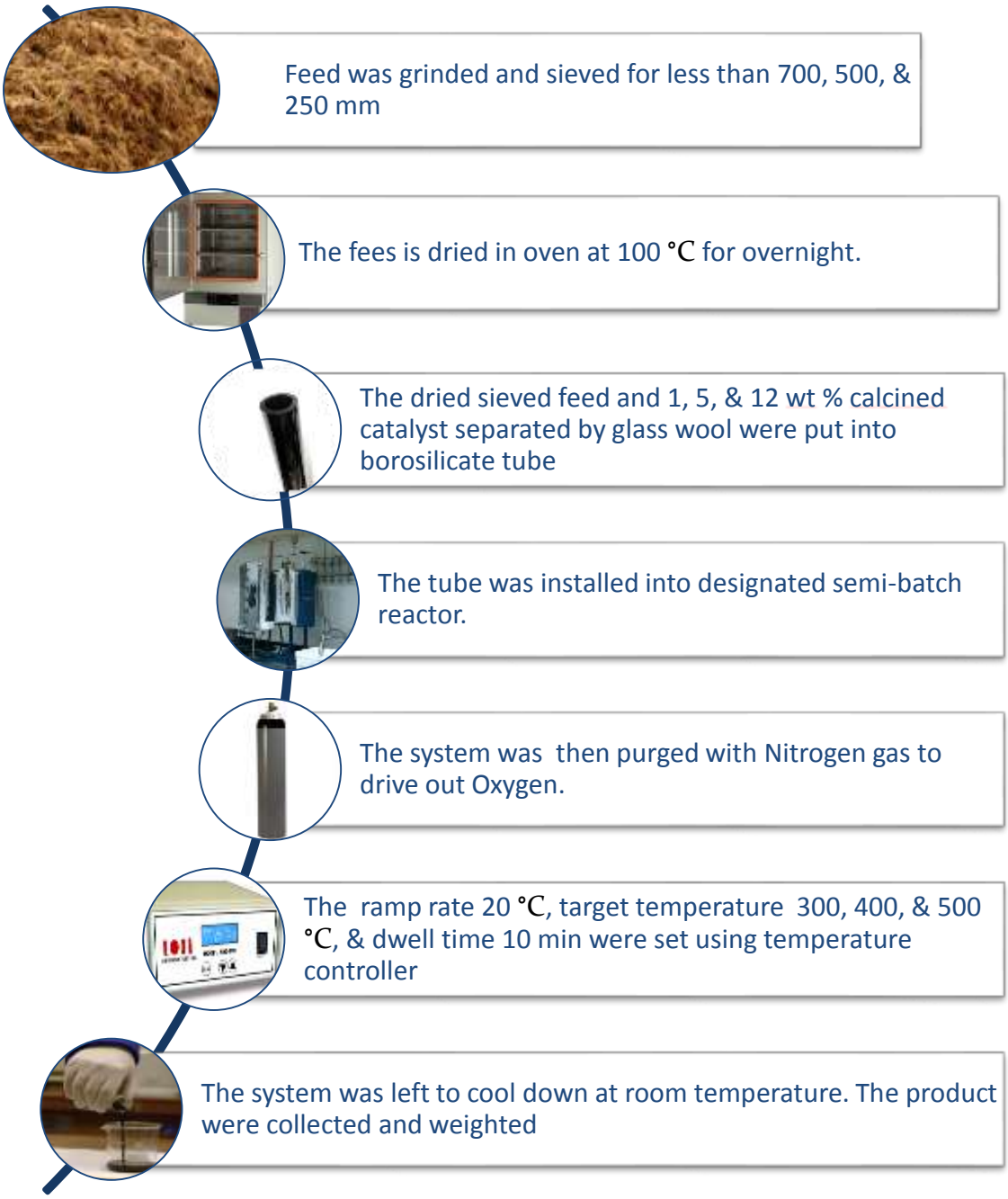

Figure 6: Slow Catalytic pyrolysis

CHAPTER 4

RESULT AND DISCUSSION

4.1 Catalyst Characterization

4.1.1 **Transmission electron microscopy** (**TEM**)

The following TEM images for nickel oxide at different reaction temperature 150 ºC, 170 ºC, and 190 ºC, calcined at 400 ºC.

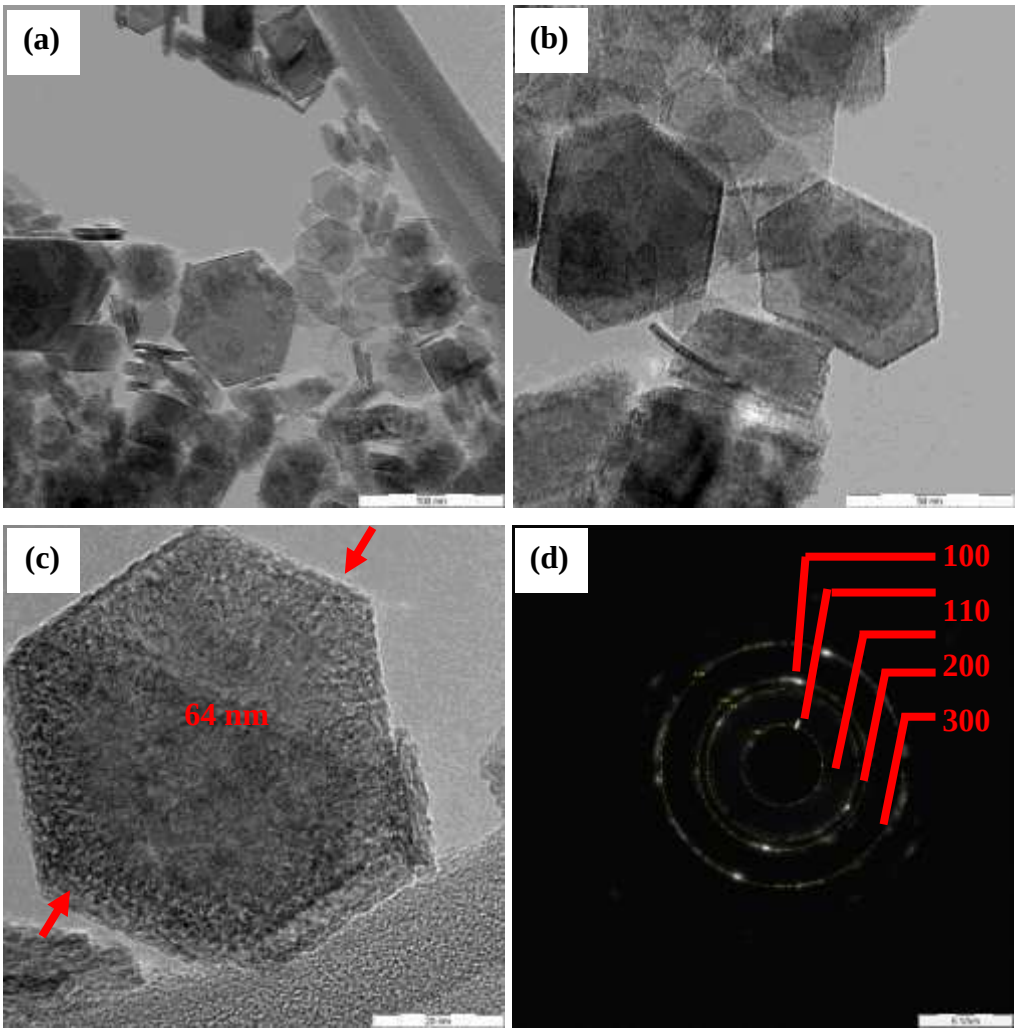

Figure 7: TEM for NiO at 150 ºC reaction temperature for 24 h

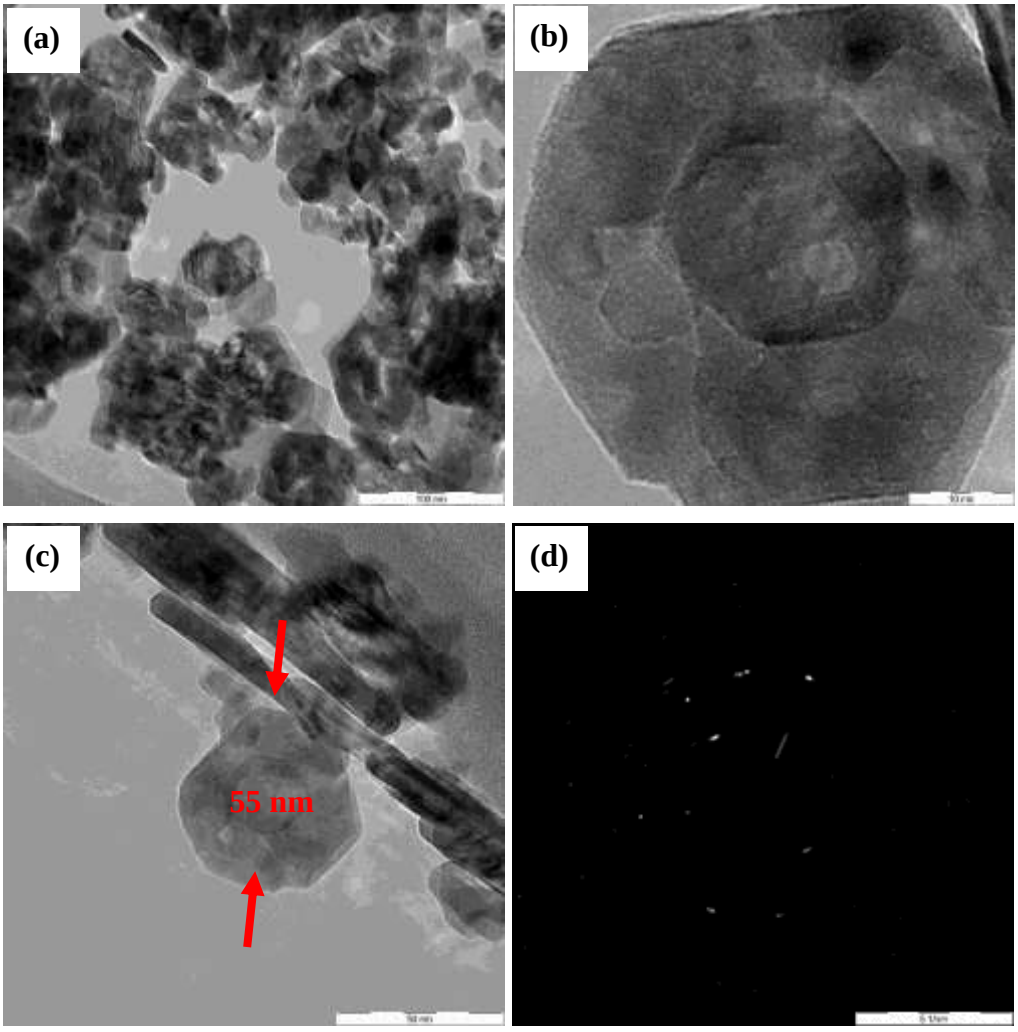

Figure 8: TEM for NiO at 170 oC reaction temperature for 24 h

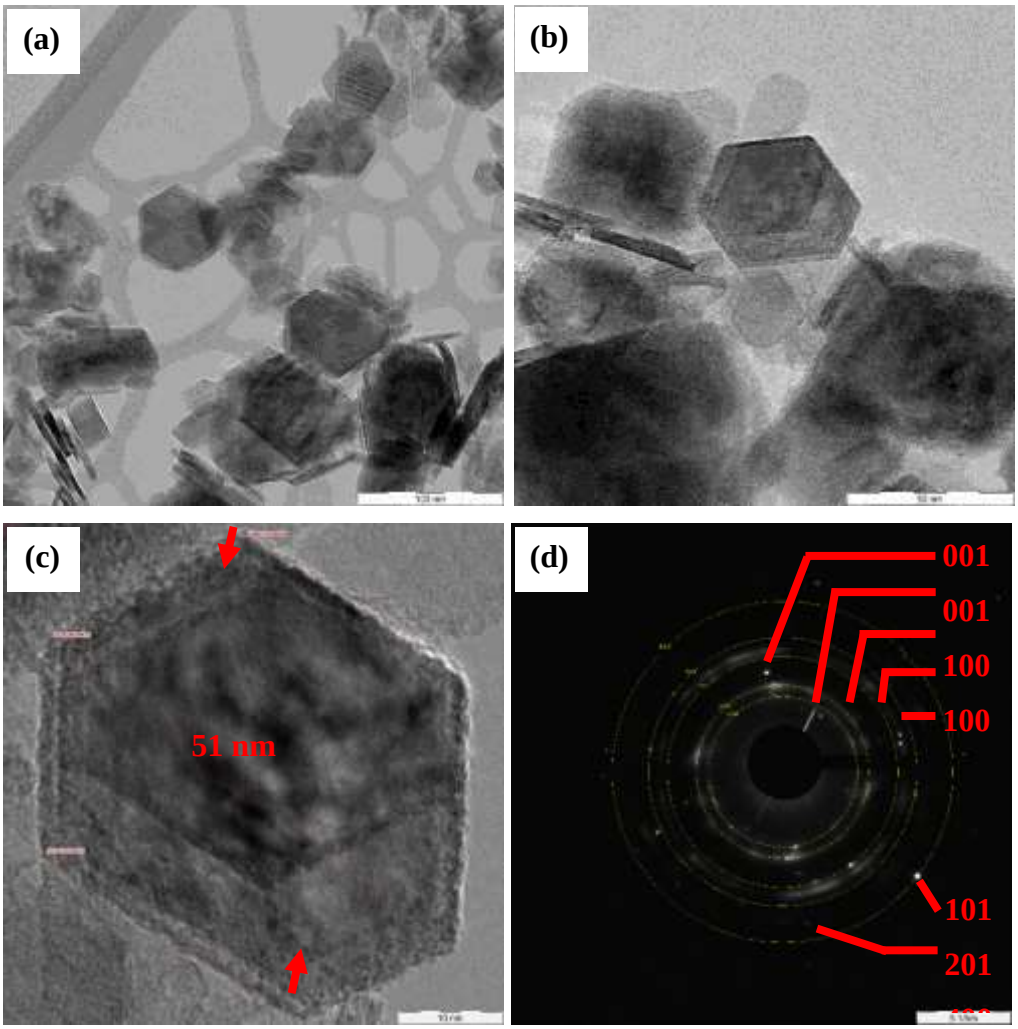

Figure 9: TEM for NiO at 190 ºC reaction temperature for 24 h

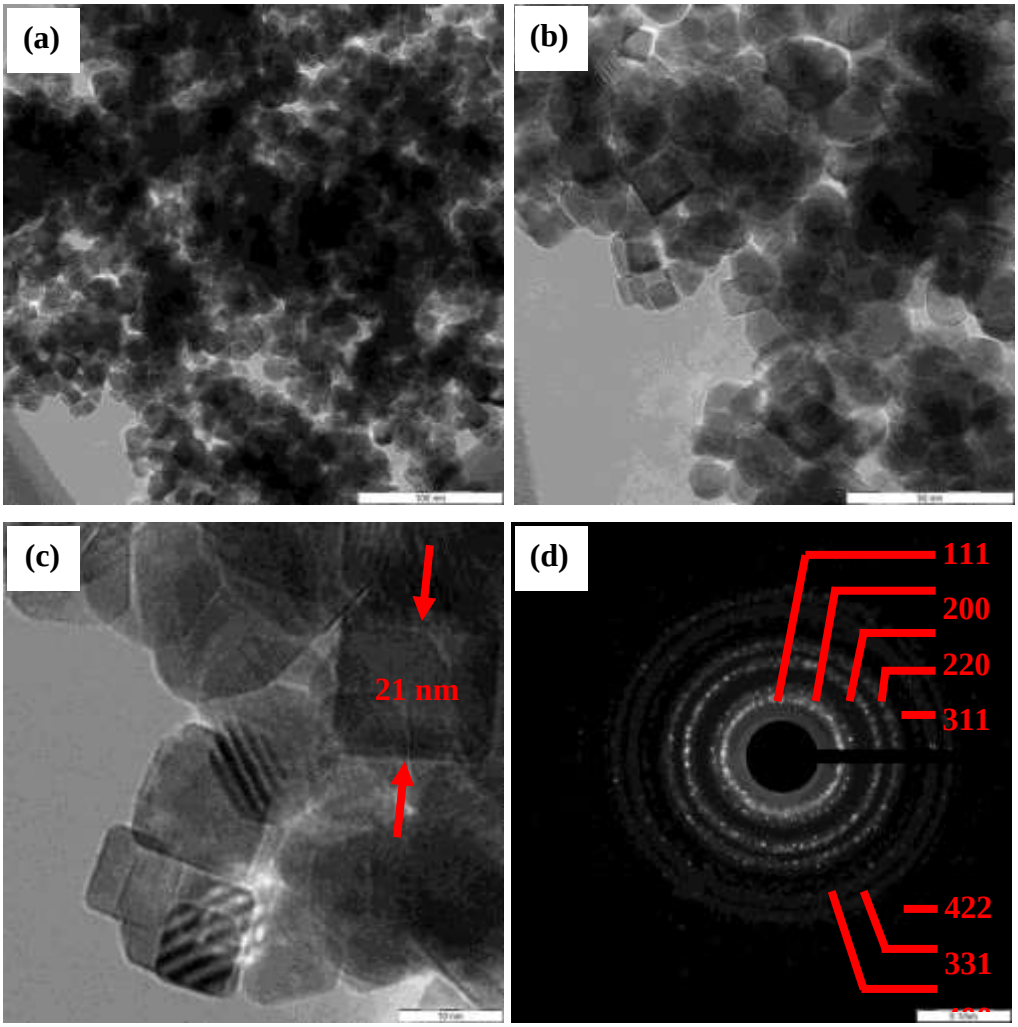

Figure 10: TEM for 10 % Fe-doped Nickel oxide

The above Figure 8, Figure 9 and figure 10 display the representative Transmission Electron Microscopy images in high resolution mode of NiO at various reaction temperature 150 oC, 170 oC and 190 oC. The interplanar spacings of NiO was determined based on the Electron Diffraction (ED) pattern ring radius as shown in Figures above before they been compared against values from the standard data (JCPDS: 34-0394). The main plane of NiO structure (2 2 0), (2 0 2) and (0 2 2) and the interaction angle of crystal face is 60o which matches they hexagonal shape crystal. Sodium hydroxide concentration play the major rule in the formation of the shape and the control of the growth on (1 1 1) along the [1 1 1]. The NiO nanosheet could for the perfect hexagonal structure, because the {2 2 0} surface energy is lower than the (1 1 1) so the Ni atomic preder to combine with oxygen atomic on the {2 2 0}. The images with lattice fringes are readily seen in tall the samples.

It is observed also that in all different reaction temperature of the synthesized NiO the nanoparticles possess a hexagonal shape. The mean size of the particles are 38 X 36 nm for 150 oC and 43 X 43 nm for 170 oC. In figure 10 it shows the TEM for 10% Fe-doped Nickel oxide which also has the hexagonal shape of the morphology. The mean size has been decreased compared to the pure nickel oxide 33 x 27 nm.

4.1.2 Scanning Electron Microscope (SEM)

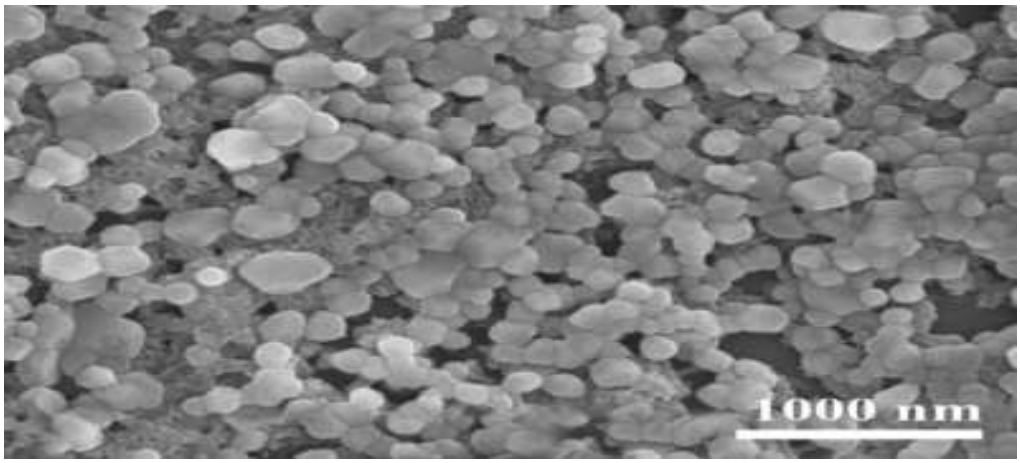

Figure 12: SEM result for Ni(OH)2

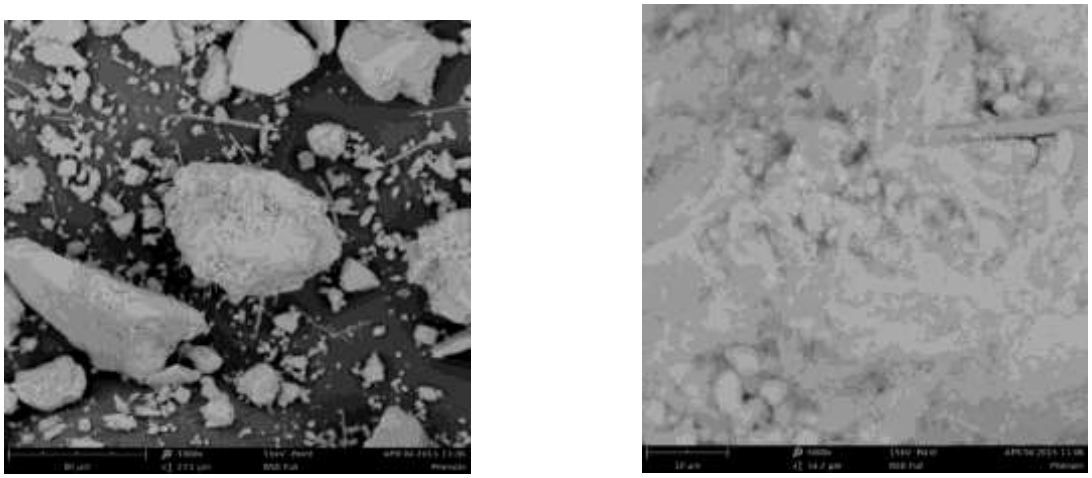

Figure 11: SEM for NiO

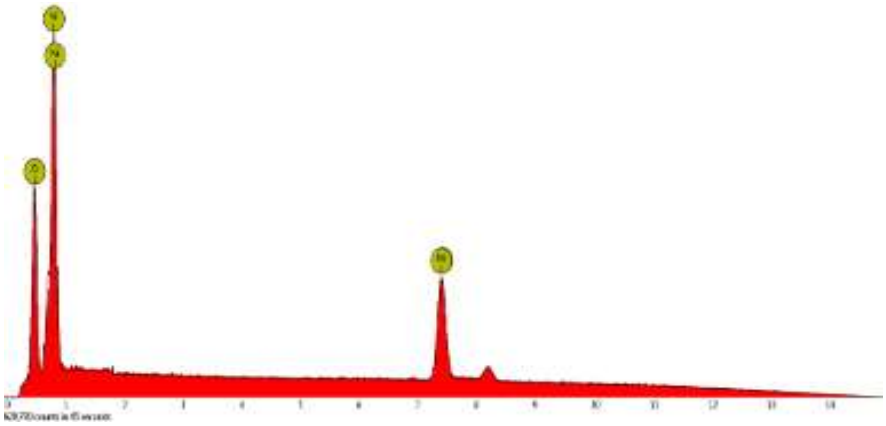

Figure 13: EDS for NiO

Table 5: EDS analysis NiO

Element Number	Element Symbol		Element Name	Weight Concentration	Error
8	O	Oxygen	26.1		0.3
28	Ni	Nickel	73.9		0.1

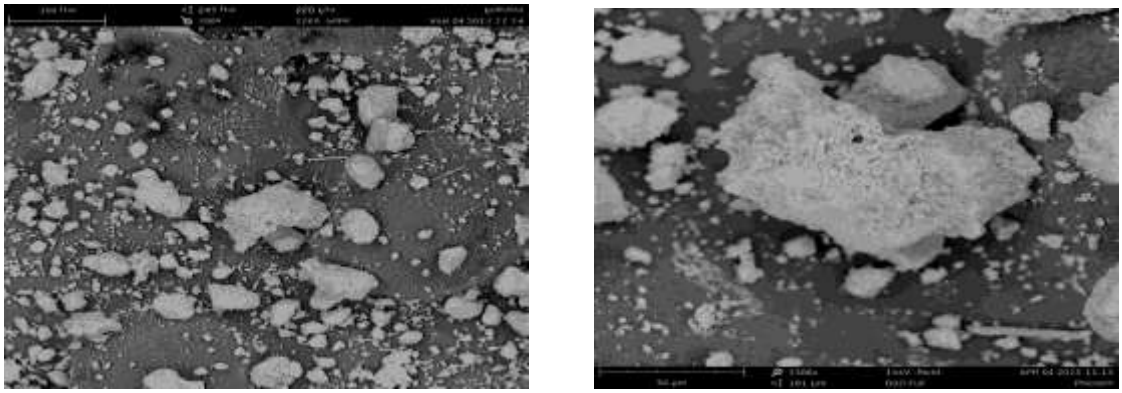

Figure 14: SEM for 10% Fe-doped NiO

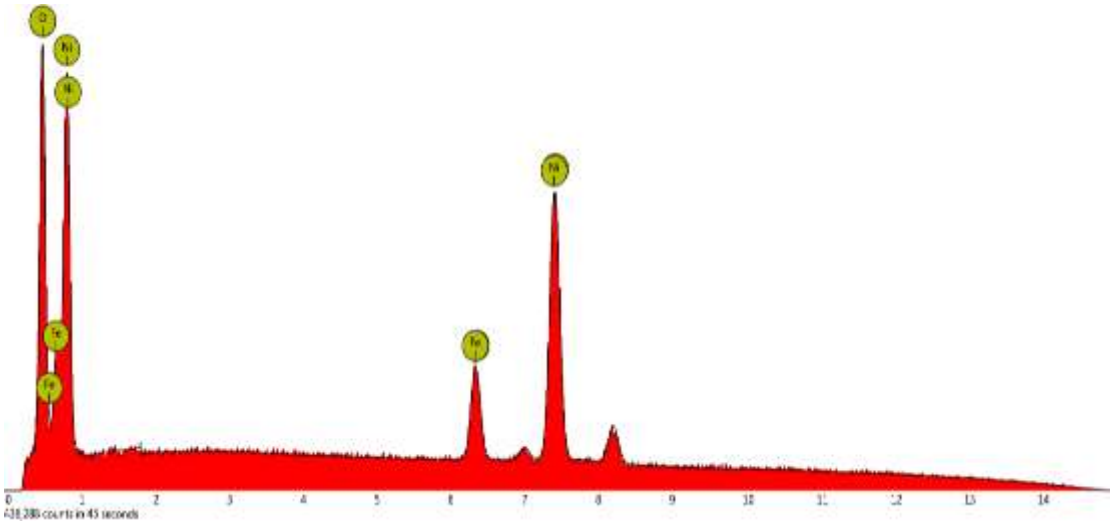

Figure 15: EDS for 10% Fe-doped Nickel Oxide

Table 6:EDS analysis for 10% Fe-doped NiO

Element Number	**Element Symbol**	**Element Name**	**Weight Concentration**	**Error**
28	Ni	Nickel	67.9	0
8	O	Oxygen	19.8	0.1
26	Fe	Iron	12.3	0.1

The Figure 16 shows that the synthesized NiO nanoparticles were quite uniform in size and Figure 17 also for the doping of iron with nickel oxide demonstrate the same shape and structure of NiO in figure 12. In both results the beaks of the elements Ni, Fe and O are obviously observed in the EDS spectrum of the sample

4.1.3 X-ray powder diffraction (XRD)

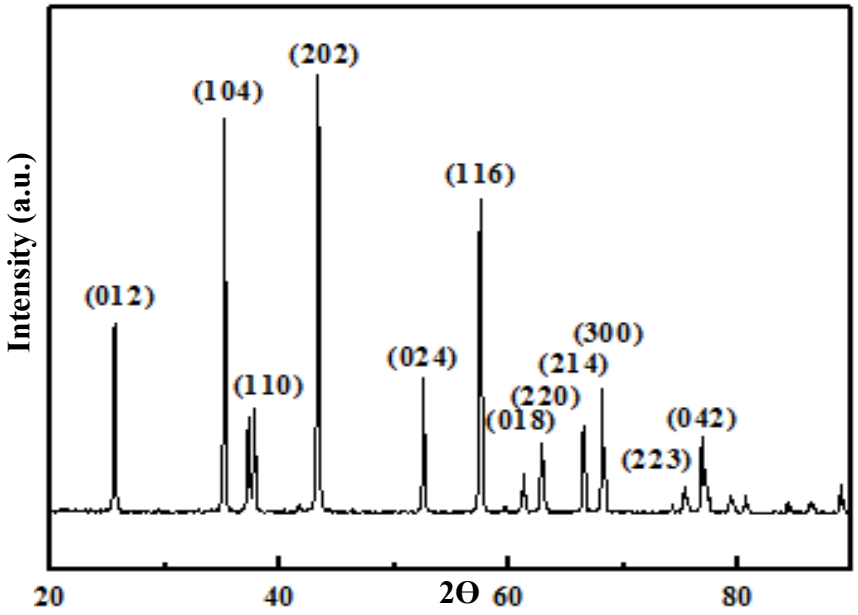

Figure 16: XRD result for Ni(OH)2 before

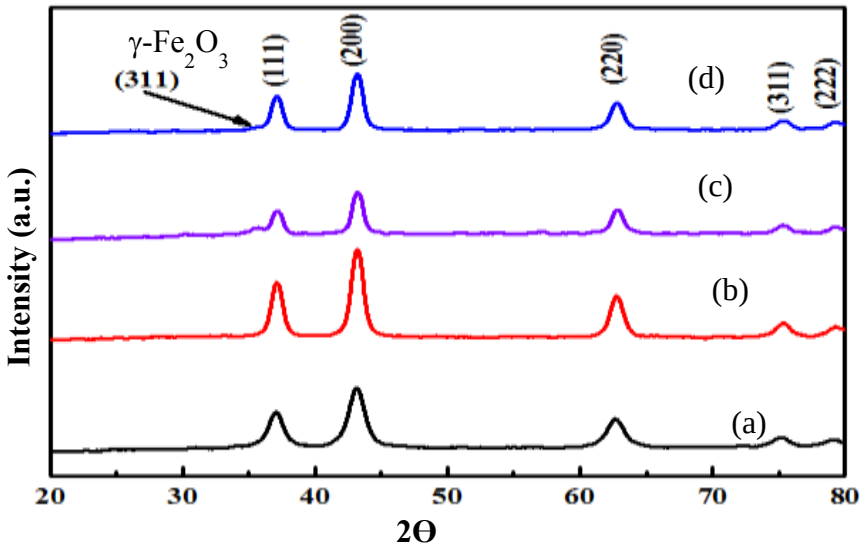

Figure 17 XRD result for(a) 0 wt% ; (b) 1wt%; (c) 5wt% and (d) 10wt% Fe-doped NiO

The XRD plots for 5% and 10% in the figure 20 (c) and (d) show that the (311) peak of γ-Fe2O3 it appears as second phase. It can also be seen that the NiO structure doesn't change on Fe doping. By comparing figure 14 which is the XRD before calcination and figure 15 after calcination it shows that synthesize of NiO was successfully transferred from for Ni(OH)2 to NiO

4.1.4 BET

Table 7: BET surface area result for NiO and Fe-doped nickel oxide

Catalyst	Fe (wt %)	Surface area m^2/g	Pore Volume cm^3/g	Pore size Å
NiO	0	121.91	0.34	11.74
1% Fe-NiO	1	37.79	0.27	286.77
5% Fe-NiO	5	35.78	0.24	264.72
10% Fe-NiO	10	32.97	0.26	307.36

The BET surface area of pure NiO and the doping of Fe with nickel oxide are shown in the above table the surface area of 121.9 m^2/g was observed for NiO. It can be observed that the surface area of the doped catalyst decreases with increasing of the loading of Iron Fe. This is due to the coverage of surface of NiO and blockage of pores by Iron.

The pure volume of the catalyst were decreases slightly with the increasing of the Iron load it also indicates the coverage of surface area and blockage of pores by Fe.

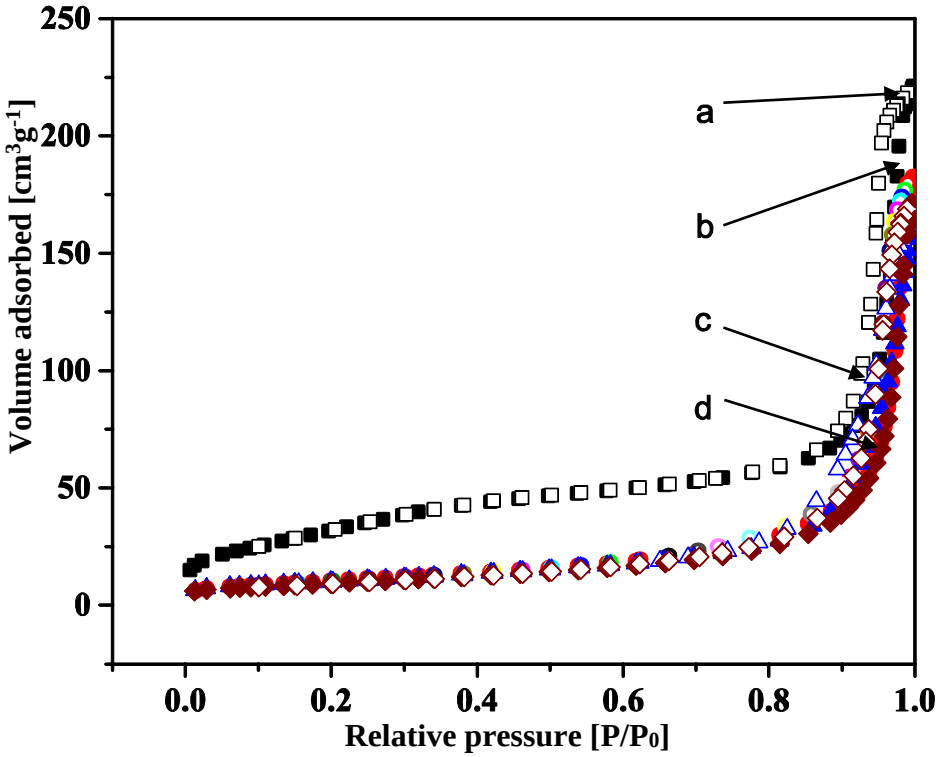

Figure 18: ASAP isotherms for(a) 0 wt% ; (b) 1wt%; (c) 5wt% and (d) 10wt% Fe-doped NiO

ASAP analysis illustrated in Fig. 19 revealed a typical IUPAC Type IV pattern featuring a mesoporous material At higher pressures the slope showed increased uptake of adsorbate as pores become filled while the inflection poin typically occurs near completion of the first monolayer.

Nickel oxide with no doping had the highest uptake adsorb volume follow by 1% Fe doped NiO. This showed a directly proportional relation to the surface area information as shown in Table

4.2 Catalytic Pyrolysis of Biomass

The slow catalytic pyrolysis experiments were performed in a semi batch reactor heated by electrical furnace as shown by Fig. 1. Dried biomass at 15.00 g and 1.5wt% (0.23 g) of catalyst were filled into a borosilicate tube separated by 2.00 g of glass wool. The borosilicate tube was tighten onto the reactor using stainless steel flange and was nitrogen-purged for 5 min at 100 ml/min to drive out all the oxygen. Next, the experiment was set at 60 ml/min with nitrogen gas supply and 400 ºC temperature with heating rate of 20 ºC/min. Vapour from the reaction was carried out by nitrogen gas and passed through a 0 ºC ice-cooled condenser to form bio oil while the remaining gas product was collected into a gas bag. The reactor was left to cool to room temperature after 10 min of experiment while maintaining the nitrogen flow. The procedure of this reaction were taken from (Dang et al., 2013)

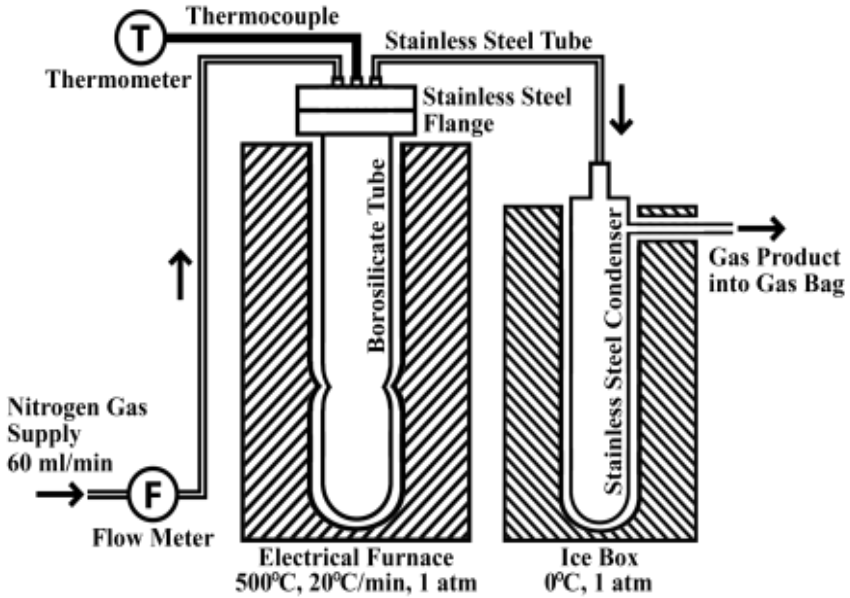

Figure 19: Schematic diagram of the process in a semi batch reactor.

The weight of the borosilicate tube including the feed and the condenser were taken before and after the experiment to measure the product yield. The bio oils produced were kept in a dark glass bottles at 3 to 5 ºC. GC analysis of the bio oil produced was performed using Agilent 7890A. The GC column used was a DB-5MS 30 m x 250 µm x 0.25 µm thickness. The oven was run at 35 ºC for 2 min, ramp at 20 ºC/min to 250 ºC, and hold for 20 min. The injector temperature was at 280 ºC and the injector split ratio was set to 83:1. The flow rate of helium carrier gas was at 100 ml/min. Bio oil samples each of 1.29 g were filtered through a 0.45 µm PTFE filter and diluted with 0.01 g of 2wt% fluroanthene internal standard solution in acetone prior to injection.

The weight of the bio char, bio oil, and gas for Run 1, 2, 3, 4, 5, and S6 were summarized in Table **8**. . The selectivity of liquid product, the product conversion, the liquid and gas yield also calculated in Table **9**. The GC analysis were used to calculate the amount of hydrogen produces in the experiments the values used to calculate the hydrogen selectivity. The following equations were used to do the

The equation used to calculate the yield are

$$\boldsymbol{W_{liquid} = W_{condenser-after} - W_{condenser-before}} \quad (1)$$

$$\boldsymbol{W_{liquid+gas} = W_{EFB} - W_{residue}} \quad (2)$$

$$\boldsymbol{Conversion = \frac{W_{gas+liquid}}{W_{EFB}}\, x100} \quad (3)$$

$$\boldsymbol{Selectivity\ of\ liquid = \frac{W_{liquid}}{W_{liquid+gas}} x100} \quad (4)$$

$$\boldsymbol{Yield_{liquid} = (selectivity\ of\ liquid\ x\ conversion)/100} \quad (5)$$

$$\boldsymbol{Yield_{gas} = conversion - Yield\ of\ liquid} \quad (6)$$

Table 8: Experimental Result

Run	Feed	Catalyst	Bio oil (g)	Bio char (g)	Gas (g)	GC Hydrogen Aria (mV/min)	Hydrogen amount (g)
1	EFB	No catalyst	5.14	5.20	4.66	125.80	0.034
2	EFB	NiO	5.80	4.92	4.32	134.51	0.033
3	EFB	1 wt % Fe-NiO	5.23	4.55	5.22	155.31	0.047
4	EFB	5 wt% Fe-NiO	5.22	4.97	4.86	236.79	0.066
5	EFB	10 wt% Fe-NiO	5.97	4.43	4.70	183.08	0.050
6	EFB	20 wt% Fe-NiO	5.53	5.01	4.48	148.99	0.038

Table 9: Experimental results of product yield.

Run	Feed	Catalyst	Conversion (%)	Bio oil selectivity (%)	Bio oil yield (%)	Gas Yield (%)	Hydrogen Selectivity (%)
1	EFB	No catalyst	69.07	49.61	34.27	31.07	0.35
2	EFB	NiO	67.47	57.31	38.67	28.80	0.33
3	EFB	1 wt% Fe-NiO	69.67	50.05	34.87	34.80	0.45
4	EFB	5 wt% Fe-NiO	67.20	51.79	34.80	32.40	0.65
5	EFB	10 wt% Fe-NiO	71.13	55.95	39.80	31.33	0.47
6	EFB	20wt% Fe-NiO	66.73	55.24	36.87	29.87	0.38

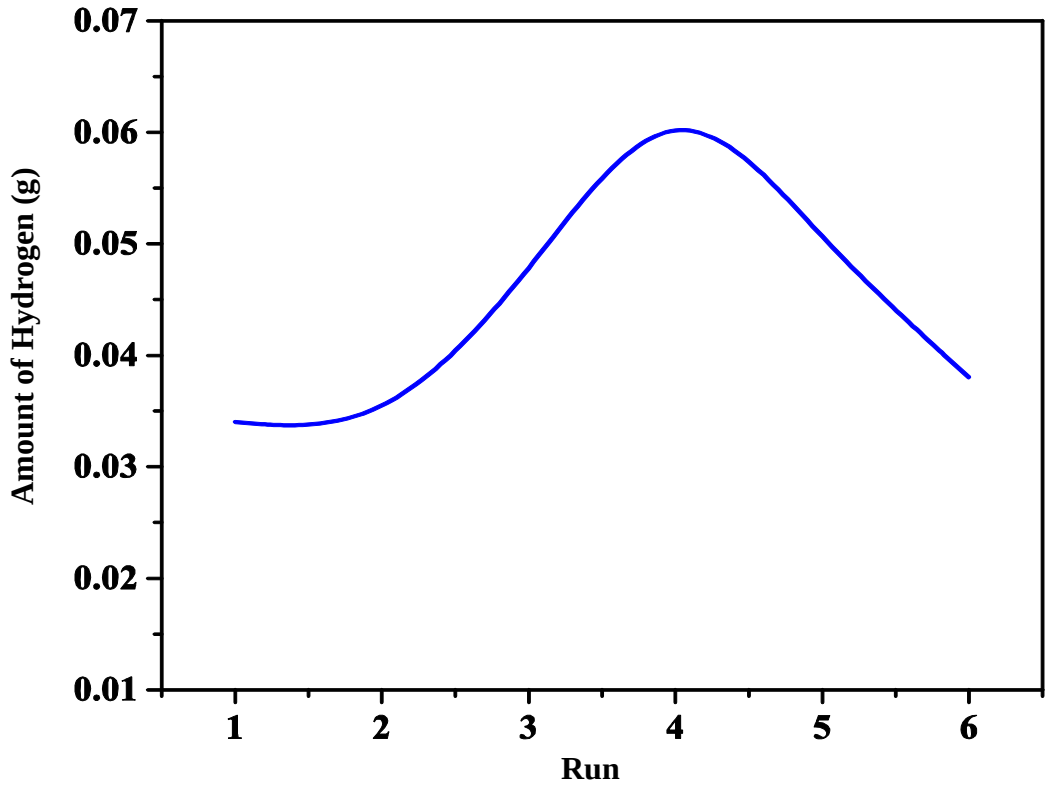

Figure 20: Amount of Hydrogen in g vs catalyst used

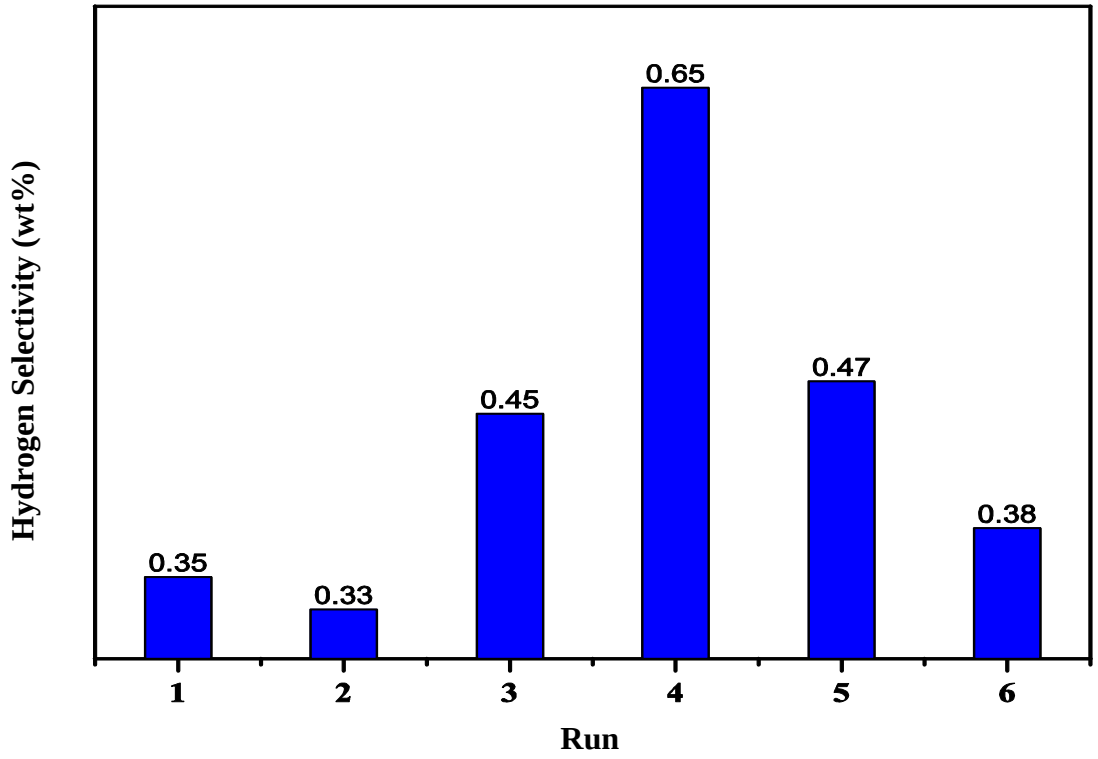

Figure 21: Hydrogen selectivity

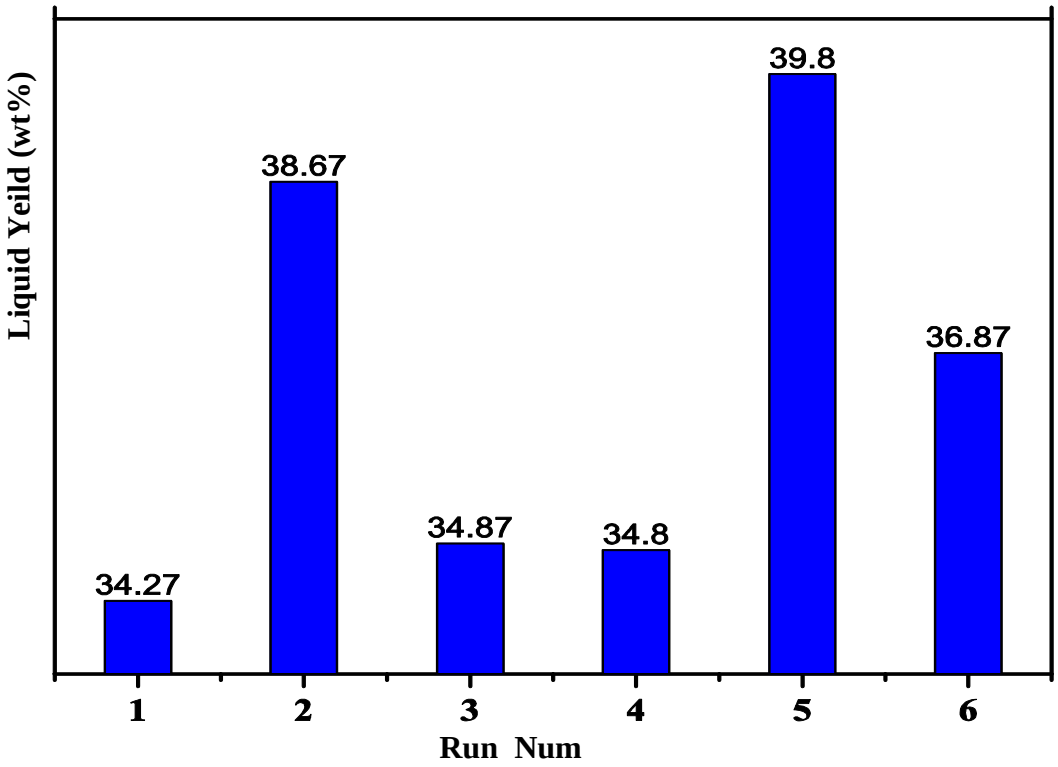

Figure 22: Yield of liquid product in condenser

Since the obtained value is above 60wt%. The conversion of pyrolysis process is high, this result shows that the pyrolysis process was successfully conducted in the developed single step reactor. The highest amount of hydrogen produced was for Run number 4 (Run 4) with selectivity of 0.65%. Run 4 represent the 5 wt% Fe-NiO

In Figure **22** the highest liquid yield of 39.8% was obtained from Run 5 which is 10 wt% Fe-NiO while the lowest liquid yield of 43.270% and 34.80% was obtained from Run 1 with no catalyst and Run 4 with 5 wt% Fe-NiO. The main reason behind the highest hydrogen production was because Iron had excellent cracking ability compared to only NiO and the optimum value was with 5 wt% doping of iron. The slow pyrolysis of Run 4 S4, as the feed produced more Gases compared to Run S5, which produces more oil.

RetTime [min]	Sig	Type	Area	Amt/Area	Amount [%]	Grp	Name
0.871	3	BB	236.78482	6.18015e-3	1.46337		Hydrogen
1.239	1	BB	122.41991	3.16058e-2	3.86918		Methane
1.379	1	BB	55.13072	1.63820e-2	9.03150e-1		Ethane
1.921	1	BB	26.32330	1.04585e-2	2.75303e-1		Propane
2.640	2	BB	2.52720e4	1.09969e-3	27.79147		Carbon dioxide
2.731	1		-	-	-		Isobutane
2.826	1	BB	9.44058	7.01799e-3	6.62539e-2		n-Butane
3.434	2	BB	79.07172	1.14262e-3	9.03493e-2		Argon
3.674	1		-	-	-		Isopentane
3.770	1		-	-	-		n-Pentane
3.988	2	BB S	4.16477e4	1.22906e-3	51.18745		Nitrogen
5.034	1		-	-	-		2,2-Dimethyl butane
Totals :					85.64653		

Figure 23: GC Hydrogen area of 5 wt%Fe-NiO

by comparing the hydrogen production resulted from the pyrolysis and cracking reaction we can observes the that the amount of hydrogen is higher and optimum when we doped 5% Fe in nickel oxide which was 0.65% selectivity compare to 0.33 which was for NiO without doping. We should consider that this values are laboratory scale and in the industrial scale the amount will be higher.

CHAPTER 5

CONCLUSION

In summary the alternative source of energy is very important because of the deleting of fossil fuel. Bio-fuel is very promising alternative being the only renewable carbon resource with sufficient short reproduction cycle Bio-oil has environmental advantages when compared to fossil fuels because , when combusted, bio-oil produces less pollution than fossil fuel

After successfully synthesized the nickel oxide catalyst with the hexagonal crystal shape and also the doping of different Wight percent of iron, the influences of factors such as type of catalyst, catalyst loading, were studied. The catalytic slow pyrolysis method was used to determine and predict the optimum concentration of Iron doped nickel oxide at the conditions of 60 ml/min of nitrogen flow rate, and temperature of 400^{o}C.

The results show the effects of the iron in producing hydrogen in the pyrolysis. The highest selectivity of hydrogen product can be observed for run number 4 with the stated above conditions and 5 wt% Fe-NiO as a catalyst for the reaction. The amount of hydrogen started to decrease as the weight percent increase after 5 wt%. The highest yield of liquid product can be observed for run number 5 with the 10 wt% Fe-doped nickel oxide.

It is expected the entire objective are achieved in this project and to be helpful and contribute goods to the society. Further work may include ceria loading onto the Fe-doped nickel oxide is possible to increase catalyst performance and enhance the cracking reaction which will produce more hydrogen.

REFERNCES

2014, B. S. R. o. W. E. J. (2014). BP Statistical Review of World Energy June 2014

Balat, M. (2011). Production of bioethanol from lignocellulosic materials via the biochemical pathway: A review. *Energy Conversion and Management, 52*(2), 858-875. doi: http://dx.doi.org/10.1016/j.enconman.2010.08.013

Bykova, M. V., Ermakov, D. Y., Kaichev, V. V., Bulavchenko, O. A., Saraev, A. A., Lebedev, M. Y., & Yakovlev, V. A. (2012). Ni-based sol–gel catalysts as promising systems for crude bio-oil upgrading: Guaiacol hydrodeoxygenation study. *Applied Catalysis B: Environmental, 113–114*(0), 296-307. doi: http://dx.doi.org/10.1016/j.apcatb.2011.11.051

Czernik, S., & Bridgwater, A. V. (2004). Overview of Applications of Biomass Fast Pyrolysis Oil. *Energy & Fuels, 18*(2), 590-598. doi: 10.1021/ef034067u

Dang, K. V., Yusup, S., Yoshimitsu, U., & Nuruddin, M. F. (2013). Catalytic Pyrolysis of Rice Husk via Semi-Batch Reactor Using L9 Taguchi Orthogonal Array. *Advanced Materials Research, 787*, 184-189.

De, S., Saha, B., & Luque, R. (2014). Hydrodeoxygenation processes: Advances on catalytic transformations of biomass-derived platform chemicals into hydrocarbon fuels. *Bioresource Technology*(0). doi: 10.1016/j.biortech.2014.09.065

Huber, G. W., Iborra, S., & Corma, A. (2006). Synthesis of transportation fuels from biomass: chemistry, catalysts, and engineering. *Chemical reviews, 106*(9), 4044-4098.

Inaba, M., Murata, K., Saito, M., & Takahara, I. (2006). Hydrogen production by gasification of cellulose over Ni catalysts supported on zeolites. *Energy & Fuels, 20*(2), 432-438.

Mann, M., Chornet, E., Czernik, S., & Wang, D. (1994). Biomass to Hydrogen via Pyrolysis and Reforming. *PREPRINTS OF PAPERS-AMERICAN CHEMICAL SOCIETY DIVISION FUEL CHEMISTRY, 39*, 1034-1034.

McKendry, P. (2002). Energy production from biomass (part 1): overview of biomass. *Bioresource Technology, 83*(1), 37-46.

Moura, K., Lima, R., Jesus, C., Duque, J., & Meneses, C. (2012). Fe-doped NiO Nanoparticles: Synthesis, Characterization, and Magnetic Properties. *Revista Mexicana de Fısica S, 58*(2), 167-170.

Sorrell, S., Speirs, J., Bentley, R., Brandt, A., & Miller, R. (2010). Global oil depletion: A review of the evidence. *Energy Policy, 38*(9), 5290-5295. doi: http://dx.doi.org/10.1016/j.enpol.2010.04.046

Sudiyani, Y., Styarini, D., Triwahyuni, E., Sudiyarmanto, Sembiring, K. C., Aristiawan, Y., . . . Han, M. H. (2013). Utilization of Biomass Waste Empty Fruit Bunch Fiber of Palm Oil for Bioethanol Production Using Pilot–Scale Unit. *Energy Procedia, 32*(0), 31-38. doi: http://dx.doi.org/10.1016/j.egypro.2013.05.005

van Ruijven, B., van Vuuren, D. P., & de Vries, B. (2007). The potential role of hydrogen in energy systems with and without climate policy. *International Journal of Hydrogen Energy, 32*(12), 1655-1672. doi: http://dx.doi.org/10.1016/j.ijhydene.2006.08.036

Wang, L., Li, D., Koike, M., Watanabe, H., Xu, Y., Nakagawa, Y., & Tomishige, K. (2013). Catalytic performance and characterization of Ni–Co catalysts for the steam reforming of biomass tar to synthesis gas. *Fuel, 112*(0), 654-661. doi: http://dx.doi.org/10.1016/j.fuel.2012.01.073

White, J. E., Catallo, W. J., & Legendre, B. L. (2011). Biomass pyrolysis kinetics: A comparative critical review with relevant agricultural residue case studies. *Journal of Analytical and Applied Pyrolysis, 91*(1), 1-33.

Yakovlev, V. A., Khromova, S. A., Sherstyuk, O. V., Dundich, V. O., Ermakov, D. Y., Novopashina, V. M., . . . Parmon, V. N. (2009). Development of new catalytic systems

for upgraded bio-fuels production from bio-crude-oil and biodiesel. *Catalysis Today, 144*(3-4), 362-366.

Zhang, X., Wang, T., Ma, L., Zhang, Q., & Jiang, T. (2013). Hydrotreatment of bio-oil over Ni-based catalyst. *Bioresource Technology, 127*(0), 306-311. doi: http://dx.doi.org/10.1016/j.biortech.2012.07.119

Appendixes

Calculations

Iron doped nickel oxide

Iron Fe	26 g/mol
Iron(III) nitrate $Fe(NO_3)_3.9H_2O$	403.999 g/mol
Nickel(II) oxide NiO	74.69 g/mol

1% Iron

$1g\ NiO$

$0.1\ wt\ \%\ Fe = \frac{0.01}{26}$

$= 0.0003846\ mol$
$= 0.0003846 * 403.999(\ \mathrm{Iron(III)nitrate})$
$= 0.15538\ g$

5% Iron

$1g\ NiO$

$5\ wt\%\ Fe = \frac{0.05}{26}$

$= 0.001923\ mol$
$= 0.001923 * 403.999(\ \mathrm{Iron(III)nitrate})$
$= 0.7769\ g$

10% Iron

$1g\ NiO$

$10\ wt\%\ Fe = \frac{0.1}{26}$

$= 0.003846\ mol$
$= 0.003846 * 403.999(\ Iron(III)nitrate)$
$= 1.5538\ g$